

GAUSSIAN PROCESS FRAMEWORK FOR TEMPORAL DEPENDENCE AND DISCREPANCY FUNCTIONS IN RICKER-TYPE POPULATION GROWTH MODELS

BY MARCELO HARTMANN^{*,1,2}, GEOFFREY R. HOSACK[†],
RICHARD M. HILLARY[†] AND JARNO VANHATALO^{*,1,2}
University of Helsinki^{} and CSIRO Marine Laboratories[†]*

Density dependent population growth functions are of central importance to population dynamics modelling because they describe the theoretical rate of recruitment of new individuals to a natural population. Traditionally, these functions are described with a fixed functional form with temporally constant parameters and without species interactions. The Ricker stock-recruitment model is one such function that is commonly used in fisheries stock assessment. In recent years, there has been increasing interest in semiparametric and temporally varying population growth models. The former are related to the general statistical approach of using semiparametric discrepancy functions, such as Gaussian processes (GP), to model deviations around the expected parametric function. In the latter, the reproductive rate, which is a key parameter describing the population growth rate, is assumed to vary in time. In this work, we introduce how these existing Ricker population growth models can be formulated under the same statistical approach of hierarchical GP models. We also show how the time invariant semiparametric approach can be extended and combined with the time varying reproductive rate using a GP model. Then we extend these models to the multispecies setting by incorporating cross-covariances among species with a continuous time covariance structure using the linear model of coregionalization. As a case study, we examine the productivity of three Pacific salmon populations. We compare the alternative Ricker population growth functions using model posterior probabilities and leave-one-out cross validation predictive densities. Our results show substantial temporal variation in maximum reproductive rates and reveal temporal dependence among the species, which have direct management implications. However, our results do not support inclusion of semiparametric discrepancy function and they suggest that the semiparametric discrepancy functions may lead to challenges in parameter identifiability more generally.

1. Introduction. Density dependent population growth functions, also known as stock-recruitment (SR) functions in fisheries, are of central importance to population dynamics modelling and fisheries stock assessment [Buckland et al. (2007),

Received August 2016; revised December 2016.

¹Supported by Academy of Finland (Grant 304531).

²Supported by University of Helsinki.

Key words and phrases. Model evidence, marginal likelihood, population growth, fisheries, density dependence, temporal dependence, interspecific dependence.

Kuikka et al. (2014), Hilborn and Walters (1992)]. These functions are of central focus because they describe the rate of recruitment of new individuals to the population, and so they are extensively used in studies concerning the productivity of fish stocks and other natural resources [e.g., Quinn and Deriso (1999), Myers, Mertz and Bridson (1997), Dorner, Peterman and Haeseker (2008), Newman et al. (2009), Pulkkinen and Mäntyniemi (2013), Mäntyniemi et al. (2015)]. In management applications, these functions are used to inform decision making about sustainable harvesting. The idea of harvesting the population at the (assumed time-invariant) maximum sustainable rate is a dominant approach in fisheries management (e.g., Magnuson–Stevens Act, US; the F_{msy} -driven harvest control rule, ICES; the Commonwealth Harvest Strategy Policy, Australia). The maximum reproductive rate is an important parameter of SR functions that determines this sustainable harvesting rate [Hilborn and Walters (1992), Quinn and Deriso (1999)].

Traditionally, population growth functions are derived from mechanistic models for population density dependent survival of offspring [Ricker (1954), Quinn and Deriso (1999), Brännström and Sumpter (2005)] and many alternatives have been suggested based on different assumptions of juvenile survival [see, e.g., Hilborn and Walters (1992), Brännström and Sumpter (2005)]. However, it has also been noticed that often these functions could not properly accommodate real-world scenarios, for which reason there has been increasing interest towards semiparametric population growth models in the recent years [Hillary (2012), Cadigan (2013)]. Early examples of semiparametric population growth functions include neural networks [Chen and Ware (1999), Chen and Irvine (2001)] and splines [Jost and Ellner (2000)]. Later, Munch, Kottas and Mangel (2005) used Gaussian processes [GPs, Rasmussen and Williams (2006)] to model deviations in the SR relationship around an expected parametric SR function. This is a special case of applying GPs to model discrepancies from an underlying mathematical process model through a “discrepancy function” [Kennedy and O’Hagan (2001), O’Hagan (2006)]. Sugeno and Munch (2013) used this same formalism to infer Allee effects in three herring data sets. Thorson, Ono and Munch (2014) developed a semiparametric state-space model, which also used a GP discrepancy function to compensate for model misspecification in the parametric population growth function, and suggested that the GP model improved estimates of the population growth function when the parametric function is misspecified.

A common assumption for semiparametric population growth functions is that they are time invariant [see, e.g., Chen and Irvine (2001), for an exception where the maximum reproductive rate depends on time-varying covariates]. However, time invariant functions may not sufficiently capture ecological processes that change with time [Peterman, Pyper and MacGregor (2003)]. Since semiparametric models, such as GPs, are very flexible, ignoring temporal variation may be especially problematic for predicting populations dynamics because the GP may inappropriately capture such temporal variation through a density dependent function. Similarly, the semiparametric discrepancy term, which is a function of the

population density, could also adapt to the temporal changes in productivity and lead to biased estimates for the density dependent growth under such model misspecification.

The traditional approach to account for time varying density dependence with parametric functions has been to use environmental data to describe deviations in recruit survival from the mean levels predicted by the simpler function [Hilborn and Walters (1992), Mäntyniemi et al. (2013), Maunder and Deriso (2011), Morita, Morita and Fukuwaka (2006)]. In the absence of environmental data, the temporal variation in the parameters of a density dependent growth function has been modeled with autoregressive models [Peterman, Pyper and Grout (2000), Peterman, Pyper and MacGregor (2003), Zeng et al. (2010)]. In practical applications, the temporal variation can improve predictions to account for the uncertainty in population productivity, and related management parameters such as Maximum Sustainable Yield (MSY) [Hilborn and Walters (1992)]. The temporal pattern of the varying parameters can also be used in building hypotheses about potential drivers of these fluctuations. Often the interest is in inferring the correlation in temporal variation of population growth among species or stocks. This has traditionally been done by calculating the correlation between species specific residual variations after fitting the time varying population growth models independently for each species [e.g., Dorner, Peterman and Haeseker (2008), Myers, Mertz and Bridson (1997), Peterman, Pyper and MacGregor (2003)]. Recently, Minto et al. (2014) used a multivariate autoregressive model to simultaneously infer the temporal variation and among population correlation in the parameters of the Ricker function. Thorson, Jensen and Zipkin (2014) constructed Beverton–Holt and Ricker models where the residual error is autocorrelated and the autocorrelation variance has a hierarchical structure over species.

Despite active development in population growth models there is a lack of rigorous statistical treatment and testing of these alternative approaches. More generally, there is a need for empirical evidence on the predictive performance of statistical models with semiparametric discrepancy functions and on parameter identifiability in such models [see, e.g., Brynjarsdóttir and O'Hagan (2014) for a recent study on the subject]. In this work, we address both questions. First, we introduce the alternative Ricker population growth functions under the unifying statistical approach of hierarchical GP models. This allows us to extend the existing discrete time models to the continuous time domain, combine the time invariant semiparametric approach with the time varying models and extend these models to the multispecies setting. These alternative models are then evaluated with a unique time series of SR data. Using a Bayesian approach, models are compared by calculating their posterior probabilities and leave-one-out cross validation predictive densities. Our case study examines the productivity of three co-located salmon populations of Pacific salmon, pink (*Oncorhynchus gorbuscha*), chum (*Oncorhynchus keta*) and sockeye (*Oncorhynchus nerka*), captured by a 51-year SR time series.

2. Case study data. The SR time series is from the Weaver Creek Spawning Channel, which is a controlled-flow environment located in the Fraser River system, British Columbia, Canada. The spawning channel was designed to augment a natural population of sockeye salmon (*Oncorhynchus nerka*) but is also used by pink (*Oncorhynchus gorbuscha*) and chum salmon (*Oncorhynchus keta*) [Rosberg, Scott and Rithaler (1986)]. The spawning channel was operated by the International Pacific Salmon Fisheries Commission until 1985 when operational management transferred to the Department of Fisheries and Oceans. Anadromous Pacific salmon species have different life history strategies but all spawn in freshwater with juveniles outmigrating to live in the ocean until returning to spawn at the end of their life cycle (semelparous organisms) [Burgner (1991), Healey (1991), Heard (1991)]. At Weaver Creek, sockeye and chum spawners returned every year 1965–2015 and pink salmon every other year.

The data used for our analyses are annual estimates of numbers of female spawners and outmigrating fry for the years 1965 to 2015 [DFO (2016)]. The number of spawning females was enumerated by a combination of methods including controlled entry of species and sex, visual survey and carcass counts; the number of outmigrating fry were estimated by a trap that samples 5% of fry passing a weir located at the end of the channel [Rosberg, Scott and Rithaler (1986)]. The average number of spawning females and fry was respectively 12,967 and 28 million for sockeye, 1841 and 2.6 million for chum, and 1513 and 1.3 million for pink. For sockeye and chum, the data are available for every year from 1965 to 2015 comprising of 51 time points. For pink salmon, which only return every other year, the data are available for every second year from 1965 to 2015 comprising of 26 time points. These data are noteworthy for the purposes of model comparison and hypothesis testing because they are comprised of direct estimates of the number of spawning females and fry over a period greater than 50 years. Typically SR datasets are comprised of estimates on spawning stock size and recruitment produced by fisheries stock assessment models.

3. Ricker population growth (stock-recruitment) models.

3.1. *Time-invariant models.* Since our data is fisheries data, we use the fisheries terminology and treat the population growth models under the SR modelling formalism, which describes the dependence of the recruitment to a population, $R_{j,t}$, in year t to a spawning stock size, $S_{j,t-\tau_j}$, in year $t - \tau_j$. In the presence of J populations of different species, denoted by $j \in \mathcal{J} = \{1, \dots, J\}$, the traditional time invariant single species Ricker SR-model [Ricker (1954)] can be summarized as

$$(3.1) \quad R_{j,t} = \alpha_j S_{j,t-\tau_j} e^{-\beta_j S_{j,t-\tau_j} + \varepsilon_{j,t}},$$

where α_j is the maximum reproductive rate, β_j the parameter governing density-dependence and $\varepsilon_{j,t}$ an i.i.d. random variable with the Gaussian distribution

$N(0, \sigma_j^2)$ that corresponds to uncertainty around the expected recruitment given by the Ricker model. Here, it should be noticed that we treat time as a continuous variable and allow the lag, τ_j from spawning to recruitment to depend on species. The maximum reproductive rate parameter, α_j , multiplied by the number of spawning females gives the number of outmigrating fry in the absence of density dependence, that is, at low population size relative to the amount of spawning habitat. In an earlier study, using a subset of our data [Essington, Quinn and Ewert \(2000\)](#) found little evidence to differentiate between the Ricker from two alternative parametric SR functions (a Beverton–Holt model and model with linear density dependence), so we progress only the former in this study.

However, we consider a more general form of the Ricker model (3.1) that allows for the presence of interspecific density dependence, which may arise due to competing for space or other resources. We write this in the log-linear form so that

$$(3.2) \quad y_{j,t} = \log \frac{R_{j,t}}{S_{j,t-\tau_j}} = \log \alpha_j - \sum_{j'=1}^J \beta_{j'} S_{j',t-\tau_{j'}} + \varepsilon_{j,t},$$

$$\mathbf{y}_t = \mathbf{a} - \mathbf{B}\mathbf{s}_t + \varepsilon_t,$$

where $\mathbf{y}_t = [y_{1,t}, \dots, y_{J,t}]^T$, $\mathbf{a} = [\log \alpha_1, \dots, \log \alpha_J]^T$, $\mathbf{s}_t = [S_{1,t-\tau_1}, \dots, S_{J,t-\tau_J}]^T$, $\varepsilon_t = [\varepsilon_{t,1}, \dots, \varepsilon_{t,J}]^T$ and \mathbf{B} is the matrix containing the density dependence parameters. When interspecific density dependence is not assumed, $\mathbf{B} = \text{diag}(\beta_1, \dots, \beta_J)$, but more generally \mathbf{B} would be a full matrix.

The traditional Ricker model (3.2) with diagonal \mathbf{B} and mutually independent prior distributions for the elements in \mathbf{a} and \mathbf{B} will serve as the base line model here. It will be called the *time-invariant independent species model* and denoted by M_0 . In this model, the reproductive rates of species are independent. However, in many cases, there is dependence between species through interspecific density dependence so that the matrix \mathbf{B} in (3.2) should have nonzero off-diagonals. The interspecific density dependence is plausible among the three salmon species considered in our study [[Essington, Quinn and Ewert \(2000\)](#)] for which reason we also include models with nonzero off-diagonal entries in \mathbf{B} into our model suite. The *time-invariant independent species model with interspecific density dependence* is an extension of M_0 where \mathbf{B} is a full matrix and it will be denoted by M_{0+dd} . The species specific prior distributions for the elements in \mathbf{a} and \mathbf{B} are summarized in [Table 1](#) and described in detail in [Appendix A.1](#).

3.2. *Time varying maximum reproductive rates.* [Minto et al. \(2014\)](#) extended the time invariant single species model (3.2) to a multivariate time varying SR model:

$$(3.3) \quad \mathbf{y}_t = \mathbf{a}_t + \mathbf{B}\mathbf{s}_t + \varepsilon_t,$$

TABLE 1

The priors for model parameters with species index $j \in \{\text{chum, pink, sockeye}\}$. Here, $\text{inv-}t_+$ denotes a half Student- t distribution for inverse of the parameter

Attribute	Parameter	Prior
The log of maximum reproductive rate, mean of the log of the maximum reproductive rate in time varying models	$a_{\text{sockeye}}, \mu_{a_{\text{sockeye}}}$	$N(-6.40, 0.36^2)$
	$a_{\text{pink}}, \mu_{a_{\text{pink}}}$	$N(-7.50, 0.52^2)$
	$a_{\text{chum}}, \mu_{a_{\text{chum}}}$	$N(-7.04, 0.51^2)$
Density dependence	β_j	$N_+(0, 1.03^2)$
Between species density dependence	$\mathbf{B}_{j,j'}, j \neq j'$	$N(0, 1.03^2)$
Standard deviation of the error	$\sigma_{\epsilon_j}^2$	$\log N(-0.27, 0.22)$
Magnitude of the time varying maximum reproductive rate	σ_j^2	$\log N(-0.14, 0.055)$
Length-scale of the time varying maximum reproductive rate	l_j	$\text{inv-}t_+(-0.02, 0.43, 4)$
Magnitude of the semiparametric correction	$\sigma_{a_{g1}}^2$	$\log N(-0.14, 0.055)$
Magnitude of the semiparametric correction	$\sigma_{a_{g2}}^2$	$\log N(-0.14, 0.055)$
Magnitude of the semiparametric correction	$\sigma_{a_{g3}}^2$	$\log N(-0.14, 0.055)$
Length-scale of the semiparametric correction	l_{g1}	$\text{inv-}t_+(0, 0.1, 4)$
Length-scale of the semiparametric correction	l_{g2}	$\text{inv-}t_+(0, 0.1, 4)$
Length-scale of the semiparametric correction	l_{g3}	$\text{inv-}t_+(0, 0.1, 4)$
Between species correlation of the time varying maximum reproductive rates	ρ	see Eq. (A.1)

where $\mathbf{a}_t = [a_{1,t}, \dots, a_{J,t}]^T$ follows a Gaussian Markov random walk model. In this model, the reproductive potential can vary annually. Such variation may originate from, for example, conditions that affect egg-to-fry survival. Reproductive potential may also be influenced by interannual factors that impact marine or freshwater conditions for adult spawners. For simplicity, throughout this study we treat the density dependence, \mathbf{B} , as time invariant which suggests that it is less affected by environmental stochasticity than density independence ($\alpha_j, j = 1, \dots, J$), or in other words, behavioral interactions are assumed to predominate. A natural extension of the discrete time random walk model would be a continuous time stochastic partial differential equation, which can be represented with GPs [Rasmussen and Williams (2006)]. Hence, we will denote a time varying maximum reproductive rate of a species j as a function of time so that $a_{j,t} = a_j(t)$.

By definition, a function $a_j(t)$ follows a Gaussian process if, for any finite set of points t_1, \dots, t_T , the vector of function values $[a_j(t_1) \dots a_j(t_T)]$ follows a multivariate Gaussian distribution [Rasmussen and Williams (2006)]. A GP is completely defined by its mean function, $m(t) = E(a_j(t))$ and its covariance function,

$k_a(t, t') = \text{Cov}(a_j(t), a_j(t'))$). The mean function specifies the expected value of the function at any location and the covariance function specifies how function values at different locations are correlated. In this work, we use constant mean functions since there is no prior information to suggest any functional form, such as trends, for them. There are many choices for the covariance function, such as the Matérn function which is among the most widely used in GP applications. However, in this work we describe the temporal covariance in log maximum reproductive rates with an exponential covariance function, $k_a(t, t' | \sigma_a^2, l_a) = \sigma_a^2 e^{-|t-t'|/l_a}$, which is a Matérn function with 1/2 degrees of freedom [Rasmussen and Williams (2006)]. Here, σ_a^2 is the process variance governing the magnitude of the variation in log maximum reproductive rate and l_a is the length-scale that governs how fast the log maximum reproductive rates vary.

The reason for using the exponential covariance function is that it makes our work more comparable to the earlier population growth models with time varying maximum reproductive rates. The exponential covariance function corresponds to the continuous representation of the AR(1) autoregressive model (the Ornstein–Uhlenbeck process). With length-scale, $l_a = -1/\log \phi$, where $\phi \in (0, 1)$, and equally lagged time steps it reproduces a discrete time autoregressive Markov random process of first order with autoregressive parameter ϕ . Hence, for discrete time data, a GP with the exponential covariance function would be an AR(1) counterpart of the random walk time-varying productivity model of Minto et al. (2014). We prefer the AR(1) model over the random walk model since the process generated from an AR(1) is second-order stationary and will not increase or decrease without bound. Other choices of covariance functions could be justified as well but these are not considered here.

3.2.1. *Time-varying independent species models.* Our first time varying Ricker model follows (3.3) so that \mathbf{B} is diagonal and we give mutually independent GP priors for the species specific maximum reproductive rates; that is,

$$(3.4) \quad a_j(t) \stackrel{\text{i.d.}}{\sim} \text{GP}(\mu_{a_j}, k_a(t, t' | \sigma_{a_j}^2, l_{a_j})),$$

where $\stackrel{\text{i.d.}}{\sim}$ denotes that the processes $a_1(t), \dots, a_J(t)$ are independent a priori. The parameter μ_{a_j} is the constant mean of the j th process, corresponding to a_j in the time-invariant single species models, and $k_a(t, t' | \sigma_{a_j}^2, l_{a_j})$ is the covariance function of the j th process. We use the exponential covariance function for all the species but allow their parameters to vary by species. The priors for the mean and covariance function parameters are summarized in Table 1 and treated in detail in Appendix A.1. These prior distributions are the same in all time varying models to be considered. We call this model the *time-varying independent species model* and denote it by M_1 .

We also extend the time-varying independent species model to allow interspecific density dependence. As with model $M_{0+\text{dd}}$, this is done by extending M_1 to allow nonzero off-diagonals in \mathbf{B} . This model will be denoted by $M_{1+\text{dd}}$.

3.2.2. *Common length-scale time varying joint species model.* Next, we consider a time varying model (3.3) that allows interspecific temporal dependence in the maximum reproductive rates. We assume that the vector-valued function of log maximum reproductive rates $\mathbf{a}_t = \mathbf{a}(t) : t \rightarrow [a_1(t), \dots, a_J(t)]^T$ follows a J -variate GP with mean $E(\mathbf{a}(t)) = [\mu_{a_1}, \dots, \mu_{a_J}]^T$ and a separable covariance function with common temporal correlation structure for all species, that is,

$$(3.5) \quad \text{Cov}(a_j(t), a_{j'}(t')) = \rho_{j,j'} \sigma_j \sigma_{j'} \tilde{k}_a(t, t' | l),$$

where $\tilde{k}_a(\cdot, \cdot | l) = k_a(\cdot, \cdot | \sigma^2 = 1, l)$ is a time dependent correlation function, $\rho_{j,j'}$ is the correlation between species j and j' and σ_j is the process standard deviation of species j . Hence, the covariance between maximum reproductive rates at different times depends on the correlation among species and on the difference in time. Since the temporal length-scale, l , is the same for each species in this model, the species specific reproductive rates are assumed to vary with similar speed in time. This may happen if the three species in the spawning channel are subjected to common temporally varying factors that impact their maximum reproductive rate. The correlations between species govern how the direction of the change in the reproductive rates are related and the process deviation parameters govern the magnitude of the changes. The prior distribution for the correlations is described in Appendix A.1. The same prior is used in all time varying joint species models.

The covariance function (3.5) leads to a model that allows interspecific relationships that affect the maximum reproductive potential, and hence, this model corresponds to the time-covarying productivity model of Minto et al. (2014). When interspecific density dependence is not considered (\mathbf{B} is diagonal), we call this model the *common length-scale time varying joint species model and denote it by M_2* . We consider also a common length-scale time varying joint species model with interspecific density dependence. This is otherwise the same model as M_2 but allows nonzero off-diagonals for \mathbf{B} . We will denote it by M_{2+dd} .

3.2.3. *Separate length-scale time-varying models.* The second time varying model with interspecific dependence in the maximum reproductive rates relaxes the assumption of common length-scale across species by defining the correlation structure of maximum reproductive rates with the linear model of coregionalization [Gelfand et al. (2003), Mardia and Goodall (1993)]. The *separate length-scale time-varying joint species model* is a time varying Ricker model (3.3) with diagonal \mathbf{B} and a J -variate GP prior for the maximum reproductive rates $\mathbf{a}(t)$. The mean of the process is again $E(\mathbf{a}(t)) = [\mu_{a_1}, \dots, \mu_{a_J}]^T$ but now the covariance function is

$$(3.6) \quad \text{Cov}(a_j(t), a_{j'}(t')) = \sum_{i=1}^J u_i(j, j') \tilde{k}_a(t, t' | l_i),$$

where $u_i(j, j')$ is the entry (j, j') of $U_i = L_i L_i'$, where L_i is the i th column of the Cholesky decomposition of the coregionalization matrix (covariance matrix) with

elements $\Sigma_{j,j'} = \sigma_j \sigma_{j'} \rho_{j,j'}$. Here, each species has its own temporal length-scale which means that the species specific reproductive rates vary at different rates in time. The correlations between species govern how rate fluctuations are connected to one another and the process variance parameters govern the magnitudes of the variations. This model will be denoted by M_3 . Its extension to allow interspecific density dependence (\mathbf{B} with nonzero off-diagonals) will be denoted by M_{3+dd} .

3.3. *Extension to account for discrepancies to the Ricker model.* In the semi-parametric approach by Munch, Kottas and Mangel (2005), the parametric SR model is augmented by a GP discrepancy function for the log of the SR function, that is, $\log R_t = f(S_{t-\tau})$ where $f(S_{t-\tau})$ has a GP prior whose mean is defined by the choice of the parametric SR function and whose covariance function can be chosen freely. Thorson, Ono and Munch (2014) used a squared exponential covariance function $k_g(S, S' | \sigma_{g_j}^2, l_{g_j}) = \sigma_{g_j}^2 e^{-(S-S')^2/l_{g_j}^2}$, where $\sigma_{g_j}^2$ is the process variance and l_{g_j} the length-scale parameter governing how fast the discrepancies vary with respect to the population size. Other covariance functions are also possible but, in order to keep our models comparable to their approach, we use the squared exponential covariance function as well. The priors for the parameters of the covariance function of the discrepancy functions are summarized in Table 1 and their biological rationale explained in Appendix A.1. Adding a GP discrepancy function to the time invariant Ricker model gives

$$(3.7) \quad \mathbf{y}_t = \mathbf{a} - \mathbf{B}\mathbf{s}_t + \mathbf{g}(\mathbf{s}_t) + \varepsilon_t,$$

where $\mathbf{g}(\mathbf{s}_t) = [g_1(S_{1,t}), \dots, g_J(S_{J,t})]^T$ is a vector-valued discrepancy function that corrects for possible mis-specifications in the species specific Ricker functions. In existing work, species have been treated independently, corresponding to independent priors for $a_j, j = 1, \dots, J$ and diagonal \mathbf{B} (i.e., no interspecific density dependence). Similarly, the discrepancy functions are also given independent GP priors, so that

$$(3.8) \quad g_j(S) \stackrel{\text{i.d.}}{\sim} \text{GP}(0, k_g(S, S' | \sigma_{g_j}^2, l_{g_j})).$$

We will call this model the *time-invariant independent species model with discrepancy function* and denote it by M_{0+df} . The model can be interpreted so that the discrepancy terms correct for the difference between the density dependent growth of the true population and theory of the Ricker model.

We also extend the alternative time-varying (multi-species) Ricker models to account for systematic deviations from the exact underlying Ricker functional form by extending the model (3.3) to

$$(3.9) \quad \mathbf{y}_t = \mathbf{a}_t - \mathbf{B}\mathbf{s}_t + \mathbf{g}(\mathbf{s}_t) + \varepsilon_t$$

with \mathbf{a}_t having a GP prior with one of the temporal covariance structures described above and $\mathbf{g}(\mathbf{s}_t)$ having the same GP prior as in model M_{0+df} . These time-varying

models with discrepancy functions will be denoted by M_{1+df} , M_{2+df} and M_{3+df} when the prior for \mathbf{a}_t follows the prior in M_1 , M_2 and M_3 .

In case of models with interspecific density dependence it is natural to assume that there is dependence also between the discrepancy functions. Hence, a natural extension to joint interspecific discrepancies is to consider a J -variate GP prior for the discrepancy functions. Here, we assume that each discrepancy process, $g_j(S)$, has a marginal GP prior with zero mean and squared exponential covariance function but the discrepancies are correlated between species so that

$$(3.10) \quad \text{Cov}(g_j(S), g_{j'}(S')) = \rho_{g_j, g_{j'}} \sigma_{g_j} \sigma_{g_{j'}} \tilde{k}_g(S, S'|l)$$

leading to multispecies discrepancy function. Here, the discrepancies would be similarly correlated between species as the time varying maximum reproductive rates in model M_2 . Since the discrepancy term is a function of the spawning stock biomass, and hence corresponds to discrepancy in the density dependence we only add the correlated discrepancy terms to the interspecific density dependence models M_{0+dd} , M_{1+dd} , M_{2+dd} , M_{3+dd} . We denote the resulting models with correlated discrepancy functions, respectively, by $M_{0+dd+df(c)}$, $M_{1+dd+df(c)}$, $M_{2+dd+df(c)}$, $M_{3+dd+df(c)}$. The suite of candidate models are summarised in Table 2.

TABLE 2

The comparison of the models according to their log marginal likelihood $[\log \pi(\mathbf{y}|M)]$, posterior probability $[\pi(M|\mathbf{y})]$ and leave-one-out cross-validation log predictive density (LOO-CV). $M_{.+dd}$ denotes models with interspecific density dependence and M_{i+df} denotes models with semiparametric discrepancy function

	Model	$\pi(M \mathbf{y})$	$\log \pi(\mathbf{y} M)$	LOO-CV
Time-invariant single species models	M_0	0.0016	-101.4	-60.0
	M_{0+dd}	0.0001	-103.9	-62.3
	M_{0+df}	<0.0001	-128.2	-63.9
	$M_{0+dd+df(c)}$	<0.0001	-128.7	-63.9
Time-varying single species models	M_1	<0.0001	-106.9	-38.2
	M_{1+dd}	<0.0001	-107.8	-39.8
	M_{1+df}	<0.0001	-135.9	-44.3
	$M_{1+dd+df(c)}$	<0.0001	-135.3	-45.9
Common length-scale time-varying joint species models	M_2	0.4899	-95.6	-31.9
	M_{2+dd}	0.3764	-95.9	-32.4
	M_{2+df}	<0.0001	-124.4	-38.2
	$M_{2+dd+df(c)}$	<0.0001	-125.0	-32.4
Separate length-scale time-varying joint species models	M_3	0.0802	-97.5	-30.3
	M_{3+dd}	0.0517	-97.9	-31.4
	M_{3+df}	<0.0001	-127.8	-36.0
	$M_{3+dd+df(c)}$	<0.0001	-128.1	-36.4

4. Inference and model comparison.

4.1. *Posterior inference.* For the purposes of implementation of the above models, we denote by $f_j(t, S_{j,t}) = a_j(t) - \beta_j S_{j,t}$ the latent “recruitment function” of species j . When data from species j is available, we denote by $\mathbf{y}_j = [y_{j,t_{j,1}}, \dots, y_{j,t_{j,T_j}}]^\top$ the vector of T_j observations for species j and by $\mathbf{f}_j = [f_j(t_{j,1}, S_{j,1}), \dots, f_j(t_{j,T_j}, S_{j,T_j})]^\top$ the vector of latent variables at time points $\mathbf{t}_j = [t_{j,1}, \dots, t_{j,T_j}]^\top$ with respective stock-size biomasses $\mathbf{S}_j = [S_{t_{j,1}}, \dots, S_{t_{j,T_j}}]^\top$. Furthermore, we stack the vectors \mathbf{f}_j , \mathbf{y}_j , \mathbf{t}_j , \mathbf{S}_j of each species, into vectors \mathbf{f} , \mathbf{y} , \mathbf{t} , \mathbf{S} , such that, for example, $\mathbf{f} = [\mathbf{f}_1^\top, \dots, \mathbf{f}_J^\top]^\top$, and denote $\boldsymbol{\mu}_\beta = [-\beta_1 \mathbf{S}_1^\top, \dots, -\beta_J \mathbf{S}_J^\top]^\top$ and $\mathbf{m}_a = [m_{a_1} \mathbf{1}_1^\top, \dots, m_{a_J} \mathbf{1}_J^\top]^\top$, where $\mathbf{1}_j$ is a $T_j \times 1$ vector of ones and m_{a_j} is the prior mean of μ_{a_j} [see equation (3.4) and Table 1]. Hence, we can write the joint prior for the expected log maximum reproductive rates at observation time points as $\boldsymbol{\mu}_a \sim N(\mathbf{m}_a, \Sigma_a)$, where $\boldsymbol{\mu}_a = [\mu_{a_1} \mathbf{1}_1^\top, \dots, \mu_{a_J} \mathbf{1}_J^\top]^\top$ and Σ_a is a block diagonal matrix, where block j is identical to the prior variance of μ_{a_j} , that is, the block j is $\sigma_{a_j}^2 \mathbf{1}_j \mathbf{1}_j^\top$ (although Σ_a is not positive definite if any $T_j > 1$ the resulting covariance matrix to be used in calculations and described below is).

Now, the conditional distribution of the observations and latent variables under all our models can be summarized as

$$(4.1) \quad \begin{aligned} \mathbf{y} | \mathbf{f}, V &\sim N(\mathbf{f}, V), \\ \mathbf{f} | \boldsymbol{\phi}_M, \mathbf{t}, \mathbf{S}, M &\sim N(\boldsymbol{\mu}_\beta + \mathbf{m}_a, \Sigma_a + \Sigma_M), \end{aligned}$$

where V is a diagonal matrix of process error variances, Σ_M is a model specific covariance matrix and $\boldsymbol{\phi}_M$ stands for all the parameters in the mean vectors and hyperparameters in the covariance functions for each specific model, $M \in \mathcal{M}$, where \mathcal{M} is the set of alternative models summarized in the second column of Table 2. All the considered models share the common mean structure of the latent process and the covariance matrix Σ_a . The alternative models differ only in the model specific covariance matrix Σ_M which are summarized in Appendix A.2.

Since the conditional distributions $p(\mathbf{f} | \boldsymbol{\phi}_M, \mathbf{t}, \mathbf{S}, M)$ and $p(\mathbf{y} | \mathbf{f}, V)$ are Gaussian (4.1), we can marginalize over the latent variables to work directly with the marginal posterior of the parameters and hyperparameters. Denote $\boldsymbol{\theta}_M = (V, \boldsymbol{\phi}_M)$ then

$$(4.2) \quad \pi(\boldsymbol{\theta}_M | \mathbf{y}, \mathbf{t}, \mathbf{S}, M) \propto N(\mathbf{y} | \boldsymbol{\mu}_\beta + \mathbf{m}_a, V + \Sigma_a + \Sigma_M) \pi(\boldsymbol{\theta}_M),$$

where $\pi(\boldsymbol{\theta}_M)$ denotes the joint prior distribution of hyperparameters (Table 1).

We conducted the posterior inference using Markov chain Monte Carlo (MCMC). We first sampled from (4.2) with the slice sampler [Neal (2003)] (see Appendix A.4) to obtain posterior samples $\Delta_M = \{\boldsymbol{\theta}_M^{(r)}, r = 1, \dots, N\}$ from (4.2). Given $\boldsymbol{\theta}_M$, the conditional posterior distributions of the latent function values and

the log maximum reproductive rates at any collection of time points are Gaussian. For example, given $\theta_M^{(r)}$ the conditional posterior of the vector of latent variables at observation times is $\mathbf{f}|\mathbf{y}, \mathbf{t}, \mathbf{S}, \theta_M^{(r)}, M \sim N(\tilde{\mathbf{m}}_f^{(r)}, \tilde{K}_f^{(r)})$ where

$$(4.3) \quad \begin{aligned} \tilde{\mathbf{m}}_f^{(r)} &= \mathbf{m}_a^{(r)} + \mu_\beta^{(r)} \\ &+ (\Sigma_a^{(r)} + \Sigma_M^{(r)})(\Sigma_a^{(r)} + \Sigma_M^{(r)} + V^{(r)})^{-1}(\mathbf{y} - \mathbf{m}_a^{(r)} - \mu_\beta^{(r)}) \end{aligned}$$

and

$$(4.4) \quad \begin{aligned} \tilde{K}_f^{(r)} &= (\Sigma_a^{(r)} + \Sigma_M^{(r)}) \\ &+ (\Sigma_a^{(r)} + \Sigma_M^{(r)})(\Sigma_a^{(r)} + \Sigma_M^{(r)} + V^{(r)})^{-1}(\Sigma_a^{(r)} + \Sigma_M^{(r)}). \end{aligned}$$

Hence, in order to obtain a sample from the joint posterior $p(\mathbf{f}, \theta_M|\mathbf{y}, \mathbf{t}, \mathbf{S}, M)$, we iteratively sampled from this multivariate Gaussian for each of the samples $\theta_M^{(r)} \in \Delta_M$. The posterior distribution for the log maximum reproductive rates can be solved analogously (see Appendix A.3).

We generated 6000 samples picking every fourth value ($N = 1500$) to decrease the variance of the Monte Carlo estimates and avoid autocorrelations between samples. We checked the mixing and stationarity of the sample chains using Geweke’s spectral density diagnostic [Geweke (1992)]. The models were implemented by using Matlab and they were added into GPstuff package [Vanhatalo et al. (2013)].

4.2. *Model comparison.* When applying the Bayesian framework, one should describe all aspects that appear relevant to the problem using probabilistic statements for which reason probabilities should also be used to reflect uncertainty about alternative models. The posterior probability of each model reflects its credibility among all alternative models. From the predictive point of view one should integrate over everything that is not fixed, also over the alternative models, which forms the basis of Bayesian model averaging (BMA) [Kass and Raftery (1995)]. From a hypothesis testing and management point of view one should also compare the posterior probabilities of models and assess their impact on alternative decisions. Hence, we compare the models presented above with their posterior probabilities by assuming a discrete uniform prior over them.

In this section, we suppress the notation by leaving out conditioning on \mathbf{t} and \mathbf{S} for brevity. We first calculate a model’s marginal likelihood (model evidence):

$$(4.5) \quad \pi(\mathbf{y}|M) = \int \pi(\mathbf{y}|\theta_M, M)\pi(\theta_M) d\theta_M.$$

Since the marginal likelihood (4.5) is not available in closed-form expression, we approximated it numerically by using the Laplace–Metropolis estimator [Kass and Raftery (1995), Lewis and Raftery (1997)]

$$(4.6) \quad \pi(\mathbf{y}|M) \approx (2\pi)^{d/2}|\hat{C}|^{1/2}\pi(\mathbf{y}|\hat{\theta}_M, M)\pi(\hat{\theta}_M),$$

where $\hat{\theta}_M$ maximizes $\pi(\mathbf{y}|\theta_M, M)\pi(\theta_M)$ among the posterior samples and the covariance-matrix \hat{C} is the MCMC approximation of the posterior covariance of θ_M and $d = \dim(\theta_M)$. After solving the marginal likelihood, we can calculate each model's posterior probability by using Bayes' theorem, $\pi(M|\mathbf{y}) = \pi(\mathbf{y}|M)\pi(M) / \sum_{M' \in \mathcal{M}} \pi(\mathbf{y}|M')\pi(M')$, where \mathcal{M} is the set of candidate models (Table 2) and $\pi(M) \propto 1$ denotes the prior probability of a model.

The marginal likelihood measures the prior predictive performance of a given model. As a measure of posterior predictive performance, we additionally calculated for each model the leave-one-out cross validation (LOO-CV) predictive density [Vehtari and Ojanen (2012)],

$$(4.7) \quad L_{\text{LOO}}(\mathbf{y}, M) = \sum_{i=1}^n \log \pi(y_i | \mathbf{y}_{-i}, M),$$

where n is the length of vector \mathbf{y} , y_i is the i th element of \mathbf{y} and $\mathbf{y}_{-i} = \{y_{i'} : i' \neq i, i = 1, \dots, n\}$. For most of the data points the prediction is made inside the range of the observed data set. Hence, LOO-CV measures a model's posterior predictive performance in interpolation. There is no closed form expression for the LOO-CV predictive distributions in (4.7). To avoid running MCMC for each of the LOO-CV training sets, we approximated the predictive density on the right-hand side of (4.7) by

$$\pi(y_i | \mathbf{y}_{-i}, M) \approx \frac{1}{N} \sum_{r=1}^N \pi(y_i | \mathbf{y}_{-i}, \theta_M^{(r)}, M),$$

where $\theta_M^{(r)} \in \Delta_M$ are samples from the full posterior $\pi(\theta_M | \mathbf{y}, M)$ and $\pi(y_i | \mathbf{y}_{-i}, \theta_M^{(r)}, M)$ is available under closed form expression [Sundararajan and Keerthi (2001)]. This approximation speeds up the computation of the LOO-CV predictive density and the error induced by approximating the LOO-CV posterior of hyperparameters by the full posterior $\pi(\theta_M | \mathbf{y}_{-i}, M) \approx \pi(\theta_M | \mathbf{y}, M)$, can be considered to be negligible. The posterior of the hyperparameters (i.e., the parameters of the mean and the covariance functions) is rather insensitive to leaving out one data point whereas the same cannot be assumed for the conditional posterior predictive distribution $\pi(y_i | \mathbf{y}_{-i}, \theta_M^{(r)}, M)$.

5. Results and discussion.

5.1. *Model comparison.* There is strong support for the time varying joint species models since the four models with highest posterior probability were, in decreasing order, M_2 , $M_{2+\text{dd}}$, M_3 and $M_{3+\text{dd}}$ (Table 2). There is also some evidence for interspecific density dependence since the second best model, which included interspecific interactions, had only slightly less posterior probability than

the best model. However, there was no support for adding semiparametric discrepancy functions since all models with the discrepancy function had negligible posterior probabilities, inferior log marginal likelihoods and low LOO-CV log predictive densities compared to models without this term. This indicates that correlated temporal evolution of the maximum reproductive rate is more relevant than a semiparametric discrepancy function.

Using the data from Weaver Creek spawning channel [Essington, Quinn and Ewert \(2000\)](#) found some evidence for interspecific density dependence only between chum and sockeye. Among the three species of salmon studied here, chum has the largest body-size, followed by sockeye and pink; sockeye avoid aggressive chum in the Weaver Creek spawning channel [[Rosberg, Scott and Rithaler \(1986\)](#)]. [Essington, Quinn and Ewert \(2000\)](#) hypothesized that the difference in fish body-size gives rise to spatial segregation of spawning sites between the species which would ease interspecific competition. They also showed that there was no evidence of strong competitive effects of pink or chum on sockeye, although there was some evidence of sockeye may exert density dependence on chum, and chum on pink salmon. However, density-dependence and maximum reproductive rates are highly dependent on each other [[Rose et al. \(2001\)](#)]. Our results (see Table 2) weakly support the hypothesis of interspecific density dependence since these models had almost equal posterior probabilities and LOO-CV predictive performance as the models without the interspecific density dependence.

5.2. Temporal variation in recruitment and maximum reproductive rate. To illustrate the differences between alternative models, we compared in more detail the best model, which is the time varying joint species model with common length-scale (M_2), to the time invariant single species models both with and without the discrepancy function (M_{0+df} and M_0). As expected the posterior predictive distribution for y varies in time more with M_2 than in the two other models (Figure 1). Notably, we see less predictive variance and better fit with M_2 for all time points throughout the species. This is reflected also by the posterior distributions of the parameters (Table 3). The model M_2 has the smallest error variance among these three models. The temporal length-scale in M_2 is rather long (approximately 77 years, Table 3) compared to the length of the data. This reflects the fact that the temporal changes in log maximum reproductive rates are smooth and there is a decreasing trend. The reproductive rates have dropped in late 1970s, then increased back upward until the early 1990s after which they have constantly decreased [Figure 1(d)]. The correlations between species specific log maximum reproductive rates in M_2 are high (ranging from approximately 0.75 to 0.85, Table 3) for which reason there is clear positive dependence in the maximum reproductive rate between all the three salmon species in the Weaver Creek spawning channel.

The maximum reproductive rate may change due to the merging of environmental settings and biological characteristics of the three species. The Weaver Creek

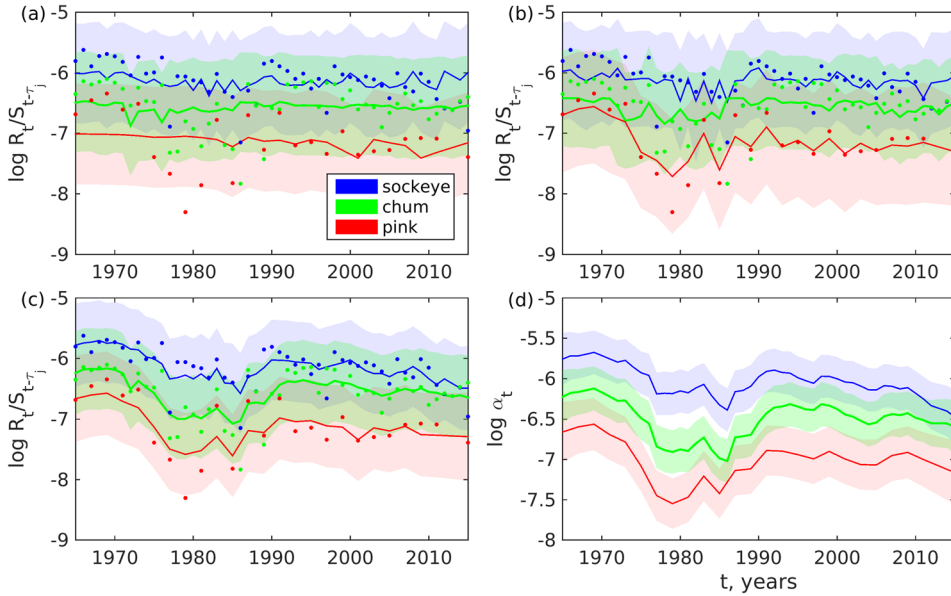


FIG. 1. The posterior predictions for $y = \log R/S$ with the time invariant single species model (M_0 , panel a), time invariant single species model with discrepancy function (M_{0+df} , panel b) and time varying joint species model with common length-scale (M_2 , panel c), and the posterior predictions for the log maximum reproductive rates $\log \alpha(t)$ in model M_2 (panel d) as a function of time. The log maximum reproductive rate in models M_0 and M_{0+df} is time invariant and their posterior distributions are summarized in Table 3. The lines show the posterior mean and the shaded area shows the posterior 95% central credible region.

channel is a controlled environment, operated to provide ideal physical reproduction habitat and to reduce variation in reproductive success due to abiotic factors [Essington, Quinn and Ewert (2000)]. Hence, we did not expect to find dramatic year to year variations in the maximum reproductive rate and our results are confirmatory in this respect (see Figure 1). Nevertheless, the time-varying models reveal two important temporal changes in the reproductivity.

The maximum reproductive rate was at a low level in the late 1970s to late 1980s, and has been constantly decreasing since the early 2000s. The former change is perhaps linked to a large flood that occurred in 1977, and to an outbreak of infectious haematopoietic necrosis virus in the late 1970s and late 1980s [Rosberg, Scott and Rithaler (1986), Traxler and Rankin (1989)], that presumably reduced outmigrating fry survival [Essington, Quinn and Ewert (2000)]. In fact, the latter study, which analysed part of the data used here, discarded several of these years as outliers, whereas our time-varying models have successfully captured such changes. In recent years, a possible explanation for decreasing maximum reproductive rates for sockeye could be explained by the trend toward early freshwater entry, which is thought to have increased pre-

TABLE 3

The posterior median (and the central posterior 95% credible interval) of the parameters under a subset of example models M_0 , M_{0+df} , M_2

Parameter	Posterior		
	M_0	M_{0+df}	M_2
$E(a_{\text{sockeye}} D)$	-5.9697	-6.0392	see Figure 1
$E(a_{\text{chum}} D)$	-6.4660	-6.5277	see Figure 1
$E(a_{\text{pink}} D)$	-7.0072	-6.9141	see Figure 1
β_{sockeye}	1.2756×10^{-5} [0.3169, 2.6703] $\times 10^{-5}$	2.2061×10^{-5} [0.3337, 7.5243] $\times 10^{-5}$	0.6757×10^{-5} [0.2455, 1.8290] $\times 10^{-5}$
β_{chum}	5.1729×10^{-5} [0.6590, 13.3550] $\times 10^{-5}$	0.8447×10^{-5} [0.5391, 29.4706] $\times 10^{-5}$	2.6466×10^{-5} [0.3545, 8.7680] $\times 10^{-5}$
β_{pink}	8.7067×10^{-5} [0.8775, 21.3320] $\times 10^{-5}$	13.7852×10^{-5} [0.9500, 48.1510] $\times 10^{-5}$	6.8499×10^{-5} [0.6727, 20.9160] $\times 10^{-5}$
σ_ϵ	0.4055 [0.3648, 0.4558]	0.3778 [0.3248, 0.4446]	0.3025 [0.2483, 0.35707]
σ_{sockeye}	-	-	0.8761 [0.6991, 1.0798]
σ_{chum}	-	-	0.9286 [0.75303, 1.1285]
σ_{pink}	-	-	0.9727 [0.7847, 1.2141]
l	-	-	77.30256 [26.1692, 241.4495]
$\sigma_{g_{\text{sockeye}}}$	-	0.8934 [0.7075, 1.1233]	-
$\sigma_{g_{\text{chum}}}$	-	0.9118 [0.7184, 1.1610]	-
$\sigma_{g_{\text{pink}}}$	-	0.8290 [0.6552, 1.0744]	-
$l_{g_{\text{sockeye}}}$	-	64979.1759 [3244.1718, 8243.9756]	-
$l_{g_{\text{chum}}}$	-	2407.3727 [749.0252, 7621.6811]	-
$l_{g_{\text{pink}}}$	-	42.9398 [1.3890, 5575.1189]	-
$\rho_{\text{sockeye, chum}}$	-	-	0.8076 [0.0250, 0.9873]
$\rho_{\text{sockeye, pink}}$	-	-	0.7567 [-0.0694, 0.9892]
$\rho_{\text{chum, pink}}$	-	-	0.8569 [0.2071, 0.9928]

spawning mortality rates [Cooke et al. (2004)]. The early entry may increase pre-spawning mortality rates because of longer exposure to high freshwater temperatures above physiological tolerances and also increased exposure to freshwater parasites [Bradford, Lovy and Patterson (2010), Hinch et al. (2012)]. In addition, within the Fraser River system the egg retention rate by viable spawners may be depressed in years with high pre-spawning mortality (D. Lofthouse, personal communication, 9 November 2016). Both increased pre-spawning mortality and increased egg retention would lead to a lower maximum reproductive rate in recent years.

5.3. *Stock-recruitment relationship under alternative model assumptions.* The effects of time varying maximum reproductive rates and discrepancy functions to the SR-function are illustrated in Figure 2. The discrepancy function only tends to

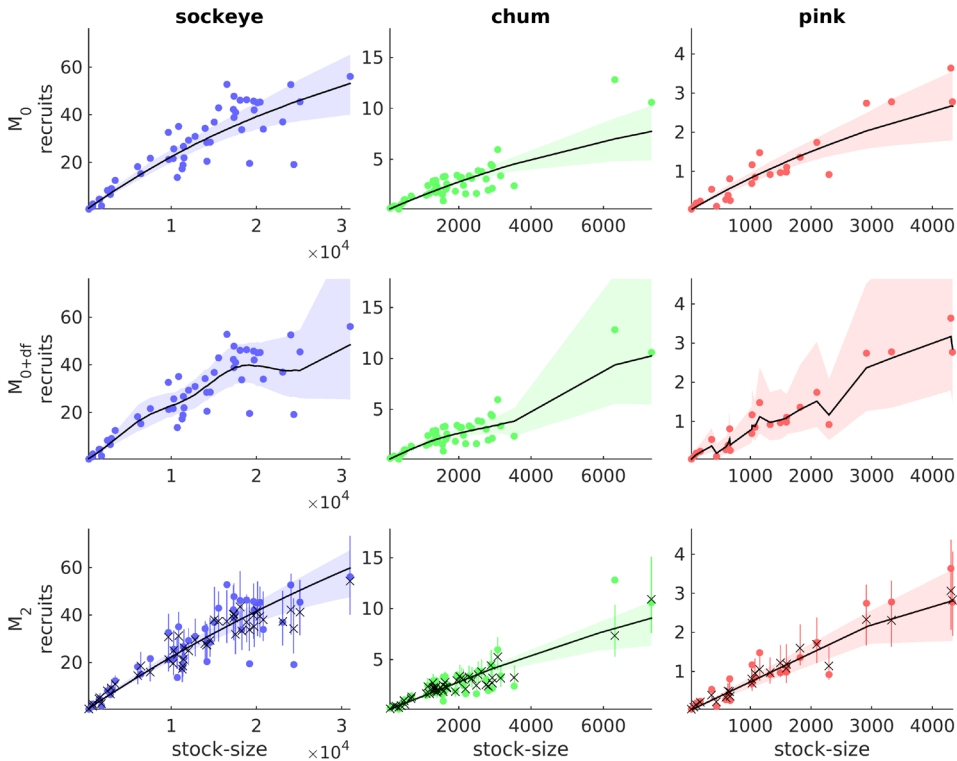


FIG. 2. The posterior probability distribution of the Ricker SR-function for the time invariant single species model (M_0), the time invariant single species model with discrepancy function (M_{0+df}) and the time varying joint species model with common length-scale (M_2). The black lines show the posterior median, the highlighted area the posterior central 95% credible interval, and the dots the data points. In the bottom row the crosses and the thin vertical lines show, respectively, the posterior median and 95% credible interval of recruits for each year from 1965 to 2015.

correct the Ricker functional form at regions where the data deviates from its expected value, which may be misleading if temporal variation in model parameters is unaccounted for. For example, in the case of sockeye the discrepancy function leads to biologically unrealistic predictions because the SR-function levels off and even decreases slightly at around 20×10^3 spawners after which it starts to increase again. Most of the data points at this region are measured between 1980 to 1985 and after 2005 when the maximum reproductive rate was low (Figure 1), for which reason the discrepancy term appears to be correcting for the time varying α .

This result is rather strong since our data were exceptionally large relative to many fisheries time series, spanning 51 years and three species, and informative since the number of spawners and recruits in the Weaver Creek are measured with higher accuracy compared to typical SR-data that are derived from stock assessment models [e.g., Minto et al. (2014)]. The addition of a discrepancy term decreased models' marginal likelihoods and the LOO-CV log predictive densities considerably compared to the base model without the discrepancy term. Although marginal likelihoods may be to some extent sensitive to chosen priors [for which we did not find evidence but see Kass and Raftery (1995)], the prior sensitivity in the LOO-CV log predictive densities with this large data is practically negligible. Hence, our results do not support using semiparametric discrepancy functions in modelling density dependent population growth in their current form, at least for the temporally extensive data.

The problem of biologically unrealistic SR-function could potentially be alleviated by defining a semiparametric discrepancy function $g(S)$ that includes monotonicity constraints. Such constraints have been used in GP models by, for example, Riihimäki and Vehtari (2010) and Brynjarsdóttir and O'Hagan (2014) who present methods to set constraints on the first derivative of a latent function. In our application, it would be natural to constrain the second derivative to be nonpositive everywhere implying that the sign of the derivative could change only once. This result is in line with the discussion by Brynjarsdóttir and O'Hagan (2014) who discuss problems with identifiability in statistical models with discrepancy functions in general. They consider similar discrepancy functions to those discussed here and in the fisheries literature and propose informative priors that set constraints on the Gaussian process discrepancy function and its derivative as a possible solution. However, we leave these considerations for the future.

5.4. Possible extensions and relationship with existing work. We presented the traditional time invariant Ricker SR-function and its extensions to include semiparametric discrepancy corrections and time varying parameters under the GP framework. The hypothesized models were evaluated with a unique 51 year empirical data set. Our results support the time varying model with species interactions but they do not support inclusion of semiparametric discrepancy functions.

Our results also add evidence to the substantial literature on the limitations of time invariant models' ability to sufficiently capture ecological processes that

change with time [e.g., Hilborn and Walters (1992), Mäntyniemi et al. (2013), Maunder and Deriso (2011), Morita, Morita and Fukuwaka (2006), Peterman, Pyper and MacGregor (2003)]. Here, we accounted for the time invariance in the productivity by building a GP model for the temporal changes in the maximum reproductive rate. Our approach can be seen as a continuous time generalization to the traditional random walk and autoregressive models [Minto et al. (2014), Peterman, Pyper and Grout (2000), Peterman, Pyper and MacGregor (2003), Zeng et al. (2010)]. Our model could straightforwardly be extended to account for environmental variables in the traditional fixed effects manner [Mäntyniemi et al. (2013), Maunder and Deriso (2011)]. In this case, the temporal GP would explain the excess temporal variation in the reproductive parameters not explainable by the known covariates.

There is growing interest in inferring correlations in time varying reproductivity between species or meta-populations (stocks in fisheries). The traditional approach has been to calculate the correlation between species specific residual variations after fitting the time varying population growth models independently for each species [e.g., Dorner, Peterman and Haeseker (2008), Myers, Mertz and Bridson (1997), Peterman, Pyper and MacGregor (2003)]. Our GP approach allows model based joint inference on these correlations. Moreover, the GP model could straightforwardly be extended to spatio-temporal setting allowing model based inference on the spatial dependence of these correlations. Such analyses have traditionally been done by fitting a parametric covariance function to the correlations between residual variations in the reproductivity in different meta-populations after fitting the time varying population growth models independently for each meta-population [e.g., Dorner, Peterman and Haeseker (2008), Myers, Mertz and Bridson (1997)]. Our approach could be extended so as to allow for joint estimation of the population growth function together with both spatial and temporal dependence.

There is also growing interest in detecting regime shifts in the productivity. For example, recently Perälä and Kuparinen (2015) built a Bayesian change point model to detect regime shifts through changes in parameters of population growth models, and Munch and Kottas (2009) used a hidden Markov model to infer regime-specific parameters and to identify regime changes. Even though our model is not specifically planned for modelling regime changes it could be extended to these applications as well by allowing the hyperparameters of the temporal processes to change in time. Note, however, that the time-varying approach allows for a rich class of continuously changing maximum reproductive values that can identify periods with high rates of change, and hence, our model can detect practical change-points.

6. Conclusions. The results contained in this paper have clear relevance to a number of key exploited population management issues. In the single-species

context, the idea of harvesting the population at the (assumed time-invariant) maximum sustainable rate still dominates in terms of management approaches globally (e.g., US Magnuson-Stevens Act, ICES the F_{msy} -driven harvest control rule, Australia the Commonwealth Harvest Strategy Policy). The maximum reproductive rate is the most dominant determinant of this sustainable harvesting rate [Hilborn and Walters (1992), Quinn and Deriso (1999)]. These results add to the already existing evidence [Minto et al. (2014)] that show that this optimal harvesting rate can be highly variable over time, with obvious implications for management approaches that assume time-invariance. In the multi-species fisheries management context, for example, the focus is almost always exclusively on the fishery, but this work shows the clear importance of the biological side of the problem. In the salmon example detailed herein, the strong temporal correlation between maximum reproductive rate, and hence, sustainable harvesting rates suggests that a sensible management approach would be to consider all three species simultaneously, not in isolation.

An important finding that has wider impact on modeling SR relationship is that the semiparametric discrepancy function adapted to temporal changes in the maximum reproductive rate (Figures 1, 2), and hence, resulted in biased estimate for the SR relationship. In fact, the unconstrained semiparametric discrepancy correction of the form given by equation (3.7) [and used, e.g., in Munch, Kottas and Mangel (2005), Sugeno and Munch (2013), Thorson, Ono and Munch (2014)] can lead to a biologically unrealistic functional form where the recruitment per spawners may level off or decrease after which it starts to increase again (Figure 2). However, a biologically reasonable restriction for SR functions is that the derivative of the SR function must be negative (if Allee effects are not considered) [Cadigan (2013)]. We therefore recommend against using unconstrained discrepancy functions to model SR functions in the presence of temporally dependent variation in the maximum reproductive rates. This result suggests also that the semiparametric discrepancy functions may lead to challenges in parameter identifiability more generally.

APPENDICES

A.1. Priors for model parameters. The priors for the (expected) log maximum reproductive rates, $\mu_{a_j} = a_j = \log \alpha_j$, are derived from the estimates of the annual fecundities, F_j , of sockeye, pink (from 1965 to 2013) and chum (from 1989 to 2013) in the Weaver Creek channel [see Essington, Quinn and Ewert (2000)] and from the estimates for mortality rates from eggs to juveniles, Q_j , of wild populations of chum, sockeye and pink [Table 1 and Figure 1 in Bradford (1995)]. The maximum reproductive rate is defined as the fecundity of a female spawner multiplied by the egg-to-fry survival probability, $\alpha_j = F_j \times s_j$, where $P_j = e^{-Q_j}$ is the egg-to-fry survival probability. We summarize the log fecundities over the study years by a Gaussian distribution with mean and variance given

by the sample mean, \hat{F}_j and sample variance, $\hat{\sigma}_{\hat{F}_j}^2$ of the log fecundity data. Similarly, we use a log-Gaussian distribution to summarize the mortality rate estimates of wild stocks by calculating its location, \hat{Q}_j and scale, $\hat{\sigma}_{\hat{Q}_j}^2$, parameters with the method of moments [Bradford (1995) provide mean estimates and standard errors]. Essington, Quinn and Ewert (2000) estimate that the survival of eggs in the Weaver Creek channel is an order of magnitude higher relative to the unmanaged Weaver Creek proper for sockeye. However, this estimate is not independent of the hatchery fry data, which were compared with the wild population to obtain the 10-fold estimate. Therefore, we did the same calculation but using estimates for sockeye in the nearest spawning channel considered by [Rosberg, Scott and Rithaler (1986), Table 52]: the Gates Creek Spawning Channel for the years 1968 to 1984. The ratio of hatchery to wild survival probabilities, ρ , was given a log-Gaussian distribution parameterised by the sample log mean, $\hat{\rho}$, (approximately 4.6) and log standard deviations, $\hat{\sigma}_{\hat{\rho}}$. This leads to a Gaussian prior distribution for $\mu_{a_j} = \log \alpha_j$ with mean $\hat{F}_j - \hat{Q}_j + \hat{\rho} - \log 10^6$ and variance $\hat{\sigma}_{\hat{F}_j}^2 + \hat{\sigma}_{\hat{Q}_j}^2 + \hat{\sigma}_{\hat{\rho}}^2$. Subtracting the factor $\log 10^6$ from these mean parameters accounts for the fact that the response is considered on the scale of millions of fry per spawning female. The induced species specific priors are given in Table 1.

We assume that positive intraspecific density dependence does not occur which induces a hard constraint $\beta_j > 0$. The parameter β is a measure of the slope of the linear relationship between spawners and the logarithm of the ratio between fry and spawners. We specify for all three species a half-Gaussian prior such that there is a 50% chance that the recruit to spawner ratio is halved given that the number of female spawners increases by 1000 individuals. This leads to a half Gaussian prior with standard deviation 1.03. For interspecific density dependence, which is described by the off-diagonal entries of \mathbf{B} , we use a Gaussian distribution with zero mean and standard deviation 1.03, which gives equal probability to positive and negative density dependence between the species, and implies that a priori the magnitude of inter-species dependence is comparable to the intra-species dependence.

In the time-invariant models M_0 , the error variance σ_j^2 can be interpreted as describing the year-to-year variation in $\log(R_j/S_j)$ given no change in S_j between years. We consider it a priori likely that, given S_j did not change, there would typically be more than two fold, but less than an order of magnitude, annual change in the ratio R_j/S_j . With $\sigma_j = 0.42$, there would be 10% probability for over two fold variation and with $\sigma_j = 1.4$, 10% chance for over an order of magnitude change. We a priori assume that once every ten years the variation would be outside these ranges. We give σ_j^2 a log-Gaussian prior with location parameter -0.27 and scale 0.22 which gives 90% probability for $0.42 < \sigma_j < 1.4$.

It is unlikely that the interannual variation in the maximum reproductive rate would exceed the natural variation (described by σ_j^2) and we assume that it is unlikely that the interannual variation is more than half of the natural variation.

Hence, we gave $\sigma_{a_j}^2$ a log-Gaussian prior with location parameter and scale parameters half and one fourth from those of σ_j . The effective range of these interannual variations is defined as the duration at which the correlation between a_t and $a_{t'}$ decays below 0.05. Temporal dependences in maximum reproductive rate greater than 5% can be induced at the population level (e.g., cohort effects) or by environmental factors (e.g., change in management around the spawning channel, ENSO, or the Pacific Decadal Oscillation). Hence, a priori it is likely that the maximum reproductive rate should either remain constant ($l = \infty$, corresponding to the base model M_0) or vary over several years; fast year to year variation should be captured by the error term, ϵ . Hence, a priori we want to favour large temporal length-scales and, in particular, we want to restrict temporal length-scales so that the maximum reproductive rate and the random variation parameters remain identifiable. With this reasoning, we defined the prior for the inverses of temporal length-scales as follows. We consider it a priori implausible that the effective range is less than 5 years and much more than 15 years. We use a heavy-tailed Student- t distribution with 4 degrees of freedom as a weakly informative prior. The location and scale parameters of the Student- t distribution were defined so that a priori the effective range is less than 5 years with probability 0.01 and greater than 15 years with probability 0.25. The choice is due to the consideration of three different kind of salmon may have different effective range and the lack of knowledge of the time dependency in the maximum reproductive rate for each specific species.

We allow the same level of variation for the discrepancy function as specified for the process variance of maximum reproductive rate. Hence, the prior for $\sigma_{a_g}^2$ is the same as that for $\sigma_{a_j}^2$. The inverse of the length-scale of the discrepancy term is given a weakly informative half Student- t prior with scale 0.1 and 4 degrees of freedom. Hence, the prior choice prefers stiff discrepancy functions with small variance (most weight is given to constant function) and is similar to the penalized complexity priors by Simpson et al. (2017). For comparison, we tried also the prior suggested by Munch, Kottas and Mangel (2005) which does not strictly follow the Bayesian reasoning since they use data to define their priors. The results were not sensitive to these choices of prior.

For the correlation matrix ρ , we assume a prior that induces marginally noninformative priors for every correlation parameters, that is, the marginal distributions for every correlation parameter ρ_{ij} is uniform over $(-1, 1)$. This is achieved by the distribution of Barnard, McCulloch and Meng (2000), Tokuda et al. (2012),

$$(A.1) \quad \pi(\rho|v) = \frac{\Gamma(\frac{v}{2})^J}{\Gamma_J(\frac{v}{2})} |\rho|^{\frac{1}{2}(v-1)(J-1)-1} \prod_{i=1}^J |\rho_{ii}|^{-\frac{v}{2}} I_{(0,\infty)}(\det \rho),$$

setting $v = J - 1$, where $\Gamma_J(x)$ is the multivariate gamma function, $|A_{ii}|$ is the determinant of a submatrix A_{ii} which is obtained by removing the i th column and i th row of A . If the parameter v increases, then the density becomes concentrated around the origin.

A.2. The structures of covariance matrices in alternative models. Within the time-invariant model, M_0 , the model specific covariance matrix is a null matrix $\Sigma_{M_0} = 0$. When interspecific density dependence is added to the time-invariant model (model M_{0+dd}) the model specific covariance matrix is $\Sigma_{M_{0+dd}} = \mathbf{D}$ where \mathbf{D} is block diagonal so that its j 'th block is $\mathbf{D}_j = \sum_{j' \neq j} \Sigma_{S_{j'}}$, where $\Sigma_{S_{j'}} = \sigma_{\beta_{j'j'}}^2 \mathbf{s}_{j'} \mathbf{s}_{j'}^T$. For the time-invariant model with discrepancy function (M_{0+df}), the model specific covariance matrix, $\Sigma_{M_{0+df}} = \mathbf{G}_{df}$, is a block diagonal matrix where the j 'th block of \mathbf{G}_{df} is constructed by the covariance function $k_{g_j}(\cdot, \cdot | \sigma_{g_j}^2, l_{g_j})$ (3.8). When both interspecies density dependence and the semiparametric discrepancy functions are present (model $M_{0+dd+df(c)}$), the model specific covariance matrix is additive so that $\Sigma_{M_{0+dd+df(c)}} = \Sigma_{M_{0+dd}} + \mathbf{G}_{df(c)}$, where $\mathbf{G}_{df(c)}$ is a full matrix of covariances $\text{Cov}(g_j(S), g_{j'}(S'))$ formed by the covariance function (3.10).

In the time-varying single species model (M_1), the model specific covariance matrix Σ_{M_1} is block diagonal so that the block j is constructed by the covariance function $k_a(\cdot, \cdot | \sigma_j^2, l_j)$ (3.3). In the models M_{1+dd} , M_{1+df} and $M_{1+dd+df(c)}$, the model specific covariance matrices are respectively $\Sigma_{M_{1+dd}} = \Sigma_{M_1} + \mathbf{D}$, $\Sigma_{M_{1+df}} = \Sigma_{M_1} + \mathbf{G}_{df}$ and $\Sigma_{M_{1+dd+df(c)}} = \Sigma_{M_1} + \mathbf{D} + \mathbf{G}_{df(c)}$.

In the common length-scale time varying joint species model (M_2), the model specific covariance matrix Σ_{M_2} is a full matrix constructed by the covariance function (3.5). Similar to the time invariant and time varying single species models, the rest of the model specific covariance matrices of the common length-scale joint species models are $\Sigma_{M_{2+dd}} = \Sigma_{M_2} + \mathbf{D}$, $\Sigma_{M_{2+df}} = \Sigma_{M_2} + \mathbf{G}_{df}$ and $\Sigma_{M_{2+dd+df(c)}} = \Sigma_{M_2} + \mathbf{D} + \mathbf{G}_{df(c)}$.

In the separate length-scale time varying joint species model (M_3), the model specific covariance matrix Σ_{M_3} is a full matrix constructed by the covariance function (3.6). Again, the rest of the model specific covariance matrices of the separate length-scale time varying joint species models are $\Sigma_{M_{3+dd}} = \Sigma_{M_3} + \mathbf{D}$, $\Sigma_{M_{3+df}} = \Sigma_{M_3} + \mathbf{G}_{df}$ and $\Sigma_{M_{3+dd+df(c)}} = \Sigma_{M_3} + \mathbf{D} + \mathbf{G}_{df(c)}$.

A.3. Posterior distribution of log maximum reproductive rates. In order to summarize the conditional posterior distributions of log maximum reproductive rates with the alternative models, we introduce a notation for four sets of models so that $\mathcal{M}_0 = \{M_0, M_{0+dd}, M_{0+df}, M_{0+dd+df(c)}\}$, $\mathcal{M}_1 = \{M_1, M_{1+dd}, M_{1+df}, M_{1+dd+df(c)}\}$, $\mathcal{M}_2 = \{M_2, M_{2+dd}, M_{2+df}, M_{2+dd+df(c)}\}$ and $\mathcal{M}_3 = \{M_3, M_{3+dd}, M_{3+df}, M_{3+dd+df(c)}\}$. Given the hyperparameter values, $\theta_M^{(r)}$, the conditional posterior of the vector of log maximum reproductive rates at observation times is multivariate Gaussian distributed, that is $\mathbf{a} | \mathbf{y}, \mathbf{t}, \mathbf{S}, \theta_M^{(r)} \sim N(\tilde{\mathbf{m}}_a^{(r)}, \tilde{K}_a^{(r)})$ where

$$(A.2) \quad \tilde{\mathbf{m}}_a^{(r)} = \mathbf{m}_a^{(r)} + (\Sigma_a^{(r)} + \Lambda_M^{(r)})(\Sigma_a^{(r)} + \Sigma_M^{(r)} + V^{(r)})^{-1}(\mathbf{y} - \mathbf{m}_a^{(r)} - \mu_\beta^{(r)})$$

$$(A.3) \quad \tilde{K}_a^{(r)} = (\Sigma_a^{(r)} + \Lambda_M^{(r)}) + (\Sigma_a^{(r)} + \Lambda_M^{(r)})(\Sigma_a^{(r)} + \Sigma_M^{(r)} + V^{(r)})^{-1}(\Sigma_a^{(r)} + \Lambda_M^{(r)})$$

and $\Sigma_M^{(r)}$ and $\Lambda_M^{(r)}$ are model specific covariance matrices. The matrix $\Sigma_M^{(r)}$ is constructed as detailed in Appendix A.2 and the matrix $\Lambda_M^{(r)}$ is constructed by the temporal covariance function of the model so that

$$(A.4) \quad \Lambda_M^{(r)} = \begin{cases} \Sigma_{M_0} & \text{if } M \in \mathcal{M}_0, \\ \Sigma_{M_1} & \text{if } M \in \mathcal{M}_1, \\ \Sigma_{M_2} & \text{if } M \in \mathcal{M}_2, \\ \Sigma_{M_3} & \text{if } M \in \mathcal{M}_3. \end{cases}$$

Hence, in order to obtain a sample from the marginal posterior $p(\mathbf{a}|\mathbf{y}, \mathbf{t}, \mathbf{S})$, we repeated sampling from this multivariate Gaussian with each of the samples in Δ_M . Similarly, if we want to predict at times not included in the training data we have

$$(A.5) \quad \tilde{\mathbf{m}}_{a_*}^{(r)} = \mathbf{m}_{a_*}^{(r)} + (\Sigma_{a_*}^{(r)} + \Lambda_{M_*}^{(r)})(\Sigma_a^{(r)} + \Sigma_M^{(r)} + V^{(r)})^{-1}(\mathbf{y} - \mathbf{m}_a^{(r)} - \mu_\beta^{(r)}),$$

$$(A.6) \quad \tilde{K}_{a_*}^{(r)} = (\Sigma_{a_*}^{(r)} + \Lambda_{M_{**}}^{(r)}) + (\Sigma_{a_*}^{(r)} + \Lambda_{M_*}^{(r)})(\Sigma_a^{(r)} + \Sigma_M^{(r)} + V^{(r)})^{-1}(\Sigma_{a_*}^{(r)} + \Lambda_{M_*}^{(r)})^T,$$

where $\Sigma_{a_*}^{(r)}$ and $\Lambda_{M_*}^{(r)}$ are covariance matrices between prediction time points (rows) and training time point (columns). $\Sigma_{a_{**}}^{(r)}$ and $\Lambda_{M_{**}}^{(r)}$ are the full covariance matrices between prediction time points.

A.4. Slice sampler scheme. To sample from (4.2), each component of the parametric vector is repeatedly sampled from its conditional posterior distribution in turn within the Gibbs sampling style. The procedure is as follows. Initialize the algorithm by choosing an initial value $\theta^{(0)}$ and setting $r = 0$. For $k = 1, \dots, \dim(\theta)$, sample $\theta_k^{(r+1)}$ from its conditional posterior distribution with the slice sampler method [Neal (2003)], that is, draw

$$(A.7) \quad \theta_k^{(r+1)} \sim \pi(\theta_k | \theta_{-k}^*, \mathbf{y}, \mathbf{S}, \mathbf{t}),$$

where $\theta_{-k}^* = \{\theta_1^{(r+1)}, \dots, \theta_{k-1}^{(r+1)}, \theta_{k+1}^{(r)}, \dots, \theta_{\dim(\theta)}^{(r)}\}$ contains all the other parameters than θ_k at their current values. Next, increment r by 1 and repeat the sample scheme until the desired sample size. We transformed parameters whose support did not cover the whole real line so that the sampling was conducted on the real line. We used log transformation for parameters that were restricted to positive real line and the correlation parameters were transformed using $\rho_{j,j'}(x_{j,j'}) = 2/[1 + \exp(-ax_{j,j'})] - 1$ where a is a positive scalar which stretches or squeeze the real line and $x_{j,j'} \in \mathcal{R}$.

Acknowledgments. The authors thank Doug Lofthouse, Carrie Holt, M. Rahikainen, T. Perälä, S. Foster, J. Dambacher and S. Mäntyniemi for comments and discussions that helped improve the paper. They also thank the DFO Salmonid Enhancement Program for generously providing the raw spawner-recruit data.

REFERENCES

- BARNARD, J., MCCULLOCH, R. and MENG, X.-L. (2000). Modeling covariance matrices in terms of standard deviations and correlations, with application to shrinkage. *Statist. Sinica* **10** 1281–1311. [MR1804544](#)
- BRADFORD, M. J. (1995). Comparative review of Pacific salmon survival rates. *Can. J. Fish. Aquat. Sci.* **52** 1327–1338.
- BRADFORD, M. J., LOVY, J. and PATTERSON, D. A. (2010). Infection of gill and kidney of Fraser River sockeye salmon, *Oncorhynchus nerka* (Walbaum), by *Parvicapsula minibicornis* and its effect on host physiology. *J. Fish Dis.* **33** 769–779.
- BRÄNNSTRÖM, Å. and SUMPTER, D. J. T. (2005). The role of competition and clustering in population dynamics. *Proc. R. Soc. Lond., B Biol. Sci.* **272** 2065–2072.
- BRYNJARSDÓTTIR, J. and O’HAGAN, A. (2014). Learning about physical parameters: The importance of model discrepancy. *Inverse Probl.* **30** 114007, 24. [MR3274591](#)
- BUCKLAND, S. T., NEWMAN, K. B., FERNÁNDEZ, C., THOMAS, L. and HARWOOD, J. (2007). Embedding population dynamics models in inference. *Statist. Sci.* **22** 44–58. [MR2408660](#)
- BURGNER, R. L. (1991). Life history of sockeye salmon (*Oncorhynchus nerka*). In *Pacific Salmon Life Histories* 3–117. UBC Press, Vancouver, BC.
- CADIGAN, N. G. (2013). Fitting a non-parametric stock-recruitment model in R that is useful for deriving MSY reference points and accounting for model uncertainty. *ICES J. Mar. Sci.* **70** 56–67.
- CHEN, D. G. and IRVINE, J. R. (2001). A semiparametric model to examine stock-recruitment relationships incorporating environmental data. *Can. J. Fish. Aquat. Sci.* **58** 1178.
- CHEN, D. G. and WARE, D. M. (1999). A neural network model for forecasting fish stock recruitment. *Can. J. Fish. Aquat. Sci.* **56** 2385–2396.
- COOKE, S. J., HINCH, S. G., ANTHONY, P. F., LAPOINTE, M. F., JONES, S. R. M., MACDONALD, J. S., PATTERSON, D. A., HEALEY, M. C. and KRAAK, G. V. D. (2004). Abnormal migration timing and high en route mortality of sockeye salmon in the Fraser River, British Columbia. *Fisheries* **29** 22–33.
- DFO (2016). Department of Fisheries and Oceans. Salmonid Enhancement Program, Weaver Creek Spawning Channel. Unpublished data.
- DORNER, B., PETERMAN, R. M. and HAESEKER, S. L. (2008). Historical trends in productivity of 120 Pacific pink, chum, and sockeye salmon stocks reconstructed by using a Kalman filter. *Can. J. Fish. Aquat. Sci.* **65** 1842–1866.
- ESSINGTON, T. E., QUINN, T. P. and EWERT, V. E. (2000). Intra- and inter-specific competition and the reproductive success of sympatric Pacific salmon. *Can. J. Fish. Aquat. Sci.* **57** 205–213.
- GELFAND, A. E., KIM, H.-J., SIRMANS, C. F. and BANERJEE, S. (2003). Spatial modeling with spatially varying coefficient processes. *J. Amer. Statist. Assoc.* **98** 387–396. [MR1995715](#)
- GEWEKE, J. (1992). Evaluating the accuracy of sampling-based approaches to the calculation of posterior moments. In *Bayesian Statistics*, 4 (*Peñíscola*, 1991) 169–193. Oxford Univ. Press, New York. [MR1380276](#)
- HEALEY, M. C. (1991). Life history of chinook salmon (*Oncorhynchus tshawytscha*). In *Pacific Salmon Life Histories* 311–394. UBC Press, Vancouver, BC.
- HEARD, W. R. (1991). Life history of pink salmon (*Oncorhynchus gorbuscha*). In *Pacific Salmon Life Histories* 119–230. UBC Press, Vancouver, BC.

- HILBORN, R. and WALTERS, C. J. (1992). *Quantitative Fisheries Stock Assessment: Choice, Dynamics and Uncertainty*. Chapman & Hall, New York.
- HILLARY, R. M. (2012). Practical uses of non-parametric methods in fisheries assessment modelling. *Mar. Freshw. Res.* **63** 606.
- HINCH, S. G., COOKE, S. J., FARRELL, A. P., MILLER, K. M., LAPOINTE, M. and PATTERSON, D. A. (2012). Dead fish swimming: A review of research on the early migration and high premature mortality in adult Fraser River sockeye salmon *Oncorhynchus nerka*. *J. Fish Biol.* **81** 576–599.
- JOST, C. and ELLNER, S. P. (2000). Testing for predator dependence in predator–prey dynamics: A non-parametric approach. *Proc. R. Soc. Lond., B Biol. Sci.* **267** 1611–1620.
- KASS, R. E. and RAFTERY, A. E. (1995). Bayes factors. *J. Amer. Statist. Assoc.* **90** 773–795. [MR3363402](#)
- KENNEDY, M. C. and O’HAGAN, A. (2001). Bayesian calibration of computer models. *J. R. Stat. Soc. Ser. B. Stat. Methodol.* **63** 425–464. [MR1858398](#)
- KUIKKA, S., VANHATALO, J., PULKKINEN, H., MÄNTYNIEMI, S. and CORANDER, J. (2014). Experiences in Bayesian inference in Baltic salmon management. *Statist. Sci.* **29** 42–49. [MR3201845](#)
- LEWIS, S. M. and RAFTERY, A. E. (1997). Estimating Bayes factors via posterior simulation with the Laplace–Metropolis estimator. *J. Amer. Statist. Assoc.* **92** 648–655. [MR1467855](#)
- MÄNTYNIEMI, S., UUSITALO, L., PELTONEN, H., HAAPASAARI, P. and KUIKKA, S. (2013). Integrated, age-structured, length-based stock assessment model with uncertain process variances, structural uncertainty, and environmental covariates: Case of central Baltic herring. *Can. J. Fish. Aquat. Sci.* **1326** 1317–1326.
- MÄNTYNIEMI, S., WHITLOCK, R. E., PERÄLÄ, T. A., BLOMSTEDT, P. A., VANHATALO, J. P., RICON, M. M., KUPARINEN, A. K., PULKKINEN, H. P. and KUIKKA, S. O. (2015). General state-space population dynamics model for Bayesian stock assessment. *ICES J. Mar. Sci.* **72** 2209–2222.
- MARDIA, K. V. and GOODALL, C. R. (1993). Spatial–temporal analysis of multivariate environmental monitoring data. In *Multivariate Environmental Statistics. North-Holland Ser. Statist. Probab.* **6** 347–386. North-Holland, Amsterdam. [MR1268443](#)
- MAUNDER, M. N. and DERISO, R. B. (2011). A state–space multistage life cycle model to evaluate population impacts in the presence of density dependence: Illustrated with application to delta smelt (*Hyposmesus transpacificus*). *Can. J. Fish. Aquat. Sci.* **68** 1285–1306.
- MINTO, C., FLEMMING, J. M., BRITTEN, G. L. and WORM, B. (2014). Productivity dynamics of Atlantic cod. *Can. J. Fish. Aquat. Sci.* **71** 203–216.
- MORITA, K., MORITA, S. H. and FUKUWAKA, M.-A. (2006). Population dynamics of Japanese pink salmon (*Oncorhynchus gorbuscha*): Are recent increases explained by hatchery programs or climatic variations? *Can. J. Fish. Aquat. Sci.* **63** 55–62.
- MUNCH, S. B. and KOTTAS, A. (2009). A Bayesian modeling approach for determining productivity regimes and their characteristics. *Ecol. Appl.* **19** 527–537.
- MUNCH, S. B., KOTTAS, A. and MANGEL, M. (2005). Bayesian nonparametric analysis of stock–recruitment relationships. *Can. J. Fish. Aquat. Sci.* **62** 1808–1821.
- MYERS, R. A., MERTZ, G. and BRIDSON, J. (1997). Spatial scales of interannual recruitment variations of marine, anadromous, and freshwater fish. *Can. J. Fish. Aquat. Sci.* **54** 1400–1407.
- NEAL, R. M. (2003). Slice sampling. *Ann. Statist.* **31** 705–767. With discussions and a rejoinder by the author. [MR1994729](#)
- NEWMAN, K. B., FERNÁNDEZ, C., THOMAS, L. and BUCKLAND, S. T. (2009). Monte Carlo inference for state-space models of wild animal populations. *Biometrics* **65** 572–583. [MR2751482](#)
- O’HAGAN, A. (2006). Bayesian analysis of computer code outputs: A tutorial. *Reliab. Eng. Syst. Saf.* **91** 1290–1300.
- PERÄLÄ, T. and KUPARINEN, A. (2015). Detecting regime shifts in fish stock dynamics. *Can. J. Fish. Aquat. Sci.* **72** 1619–1628.

- PETERMAN, R. M., PYPER, B. J. and GROUT, J. A. (2000). Comparison of parameter estimation methods for detecting climate-induced changes in productivity of Pacific salmon (*Oncorhynchus spp.*). *Can. J. Fish. Aquat. Sci.* **57** 181–191.
- PETERMAN, R. M., PYPER, B. J. and MACGREGOR, B. W. (2003). Use of the Kalman filter to reconstruct historical trends in productivity of Bristol Bay sockeye salmon (*Oncorhynchus nerka*). *Can. J. Fish. Aquat. Sci.* **60** 809–824.
- PULKKINEN, H. and MÄNTYNIEMI, S. (2013). Maximum survival of eggs as the key parameter of stock-recruit meta-analysis: Accounting for parameter and structural uncertainty. *Can. J. Fish. Aquat. Sci.* **70** 527–533.
- QUINN, T. J. and DERISO, R. B. (1999). *Quantitative Fish Dynamics*. Oxford Univ. Press.
- RASMUSSEN, C. E. and WILLIAMS, C. K. I. (2006). *Gaussian Processes for Machine Learning*. MIT Press, Cambridge, MA. MR2514435
- RICKER, W. E. (1954). Stock and recruitment. *J. Fish. Res. Board Can.* **5** 559–623.
- RIIHIMÄKI, J. and VEHTARI, A. (2010). Gaussian processes with monotonicity information. *J. Mach. Learn. Res. Workshop Conf. Proc.* **9** 645–652. (AISTATS 2010 Proceedings).
- ROSBERG, G. E., SCOTT, K. J. and RITHALER, R. (1986). Review of the International Pacific Salmon Fisheries Commission's Sockeye and Pink salmon enhancement facilities on the Fraser River. Technical Report, Department of Fisheries and Oceans, Vancouver, Canada.
- ROSE, K. A., JUNIOR, J. A. C., WINEMILLER, K. O., MYERS, R. A. and HILBORN, R. (2001). Compensatory density dependence in fish populations: Importance, controversy, understanding and prognosis. *Fish Fish.* **2** 293–327.
- SIMPSON, D., RUE, H., RIEBLER, A., MARTINS, T. G. and SØRBYE, S. H. (2017). Penalising model component complexity: A principled, practical approach to constructing priors. *Statist. Sci.* **32** 1–28. MR3634300
- SUGENO, M. and MUNCH, S. B. (2013). A semiparametric Bayesian method for detecting Allee effects. *Ecology* **94** 1196–1204.
- SUNDARARAJAN, S. and KEERTHI, S. S. (2001). Predictive approaches for choosing hyperparameters in Gaussian processes. *Neural Comput.* **13** 1103–1118.
- THORSON, J. T., JENSEN, O. P. and ZIPKIN, E. F. (2014). How variable is recruitment for exploited marine fishes? A hierarchical model for testing life history theory. *Can. J. Fish. Aquat. Sci.* **983** 973–983.
- THORSON, J. T., ONO, K. and MUNCH, S. B. (2014). A Bayesian approach to identifying and compensating for model misspecification in population models. *Ecology* **95** 329–341.
- TOKUDA, T., GOODRICH, B., VAN MECHELEN, I., GELMAN, A. and TUERLINCKX, F. (2012). Visualizing distributions of covariance matrices. Technical report, University of Leuven, Belgium and Columbia University, USA. Available at <http://www.stat.columbia.edu/~gelman/research/unpublished/Visualization.pdf>.
- TRAXLER, G. and RANKIN, J. (1989). An infectious hematopoietic necrosis epizootic in sockeye salmon *Oncorhynchus nerka* in Weaver Creek spawning channel, Fraser River system, BC, Canada. *Dis. Aquat. Org.* **6** 221–226.
- VANHATALO, J., RIIHIMÄKI, J., HARTIKAINEN, J., JYLÄNKI, P., TOLVANEN, V. and VEHTARI, A. (2013). GPstuff: Bayesian modeling with Gaussian processes. *J. Mach. Learn. Res.* **14** 1175–1179. MR3063621
- VEHTARI, A. and OJANEN, J. (2012). A survey of Bayesian predictive methods for model assessment, selection and comparison. *Stat. Surv.* **6** 142–228. MR3011074
- ZENG, Z., NOWIERSKI, R. M., TAPER, M. L., DENNIS, B. and KEMP, W. P. (2010). Complex population dynamics in the real world: Modeling the influence of time-varying parameters and time lags. *Ecology* **79** 2193–2209.

M. HARTMANN
J. VANHATALO
DEPARTMENT OF MATHEMATICS AND STATISTICS
DEPARTMENT OF BIOSCIENCES
00014 UNIVERSITY OF HELSINKI
P.O. BOX 68
FINLAND
E-MAIL: marcelo.hartmann@helsinki.fi
jarno.vanhatalo@helsinki.fi

G. R. HOSACK
R. M. HILLARY
CSIRO MARINE LABORATORIES
CASTRAY ESPLANADE
HOBART, TASMANIA 7001
AUSTRALIA
E-MAIL: Geoff.Hosack@csiro.au
Rich.Hillary@csiro.au